

1 **Title:** Reactive oxygen species signalling is involved in alkamide-induced alterations in root  
2 development.

3 **Running title:** Alkamides and ROS signalling

4 Tonatiu Campos-García <sup>a, b</sup>, Jorge Molina-Torres <sup>b</sup>, and Kirk Overmyer <sup>a, #</sup>

5 <sup>a</sup> Organismal and Evolutionary Biology Research Program, Faculty of Biological and  
6 Environmental Sciences, and Viikki Plant Science Centre. University of Helsinki, P.O. Box  
7 65 (Viikinkaari 1), FI-00014 Helsinki, Finland.

8 <sup>b</sup> Departamento de Biotecnología y Bioquímica, Unidad Irapuato, Cinvestav, Irapuato,  
9 Guanajuato, México

10 <sup>#</sup>Corresponding Author: Kirk Overmyer; University of Helsinki, P.O Box 65 (Viikinkaari 1),  
11 FI-00014 Helsinki, Finland; +(358) 44 337-7528; kirk.overmyer@helsinki.fi.

12 **Date of submission:** 23 December, 2021

13 **Number of tables and figures:** 7 (6 figures and 1 table)

14 **Word count:** Total: 5212 (Introduction, 1020; Results, 1560; Discussion, 2386;  
15 Conclusions, 174; Acknowledgements 72; Materials and Methods, 971).

16

17

18

19

20

21

22

23

24 **Highlight**

25 Reactive oxygen species (ROS) are involved in alkamide-induced altered root development.  
26 Heterotrimeric G-protein complex, extracellular acidification, and ROS sourced from  
27 peroxidases and NADPH-oxidases are involved in these processes.

28 **Abstract**

29 Alkamides are alpha unsaturated *N*-acylamides structurally related to *N*-acyl ethanolamides  
30 (NAEs) and *N*-acyl-L-homoserine lactones (AHLs). Studies have shown that alkamides  
31 induce prominent changes in root architecture, a significant metabolic readjustment, and  
32 transcriptional reprogramming. Some alkamide responses have been associated with redox  
33 signalling; however, this involvement and ROS sources have not been fully described. We  
34 utilized a genetic approach to address ROS signalling in alkamide-induced processes and  
35 found that in *Arabidopsis*, treatment with the alkamide affinin (50 $\mu$ M) increased the *in-situ*  
36 accumulation of H<sub>2</sub>O<sub>2</sub> in lateral root emergence sites and reduced H<sub>2</sub>O<sub>2</sub> accumulation in  
37 primary root meristems implying that altered root growth was dependent on endogenous  
38 H<sub>2</sub>O<sub>2</sub>. Results show that ROS sourced from PRX34, RBOHC and RBOHD were involved in  
39 promotion of lateral root emergence by alkamides. RBOHC was required for affinin-induced  
40 enhanced root hair expansion. Furthermore, affinin-induced changes in lateral root  
41 emergence, but not root hair length, were dependent on a change in extracellular pH. Finally,  
42 reverse genetic experiments suggest heterotrimeric G-proteins were involved in plant  
43 response to alkamides; nevertheless, further studies with additional higher order G-protein  
44 mutants will be required to resolve this question. These results support that alkamides recruit  
45 specific ROS signaling programs to mediate alterations in root architecture.

46

47 **Keywords:** affinin, alkamides, development, lateral roots, ROS, root, root growth, reverse  
48 genetics, pH

## 49 Introduction

50 In plants and animals some metabolites interact with messengers or receptors to modulate  
51 diverse metabolic pathways and signal transduction cascades. Plant chemical effectors from  
52 different sources can trigger physiological and morphological responses. Alkamides are low  
53 molecular weight  $\alpha$ -unsaturated acyl-amide plant metabolites distributed in some plant  
54 species. These metabolites are known to have a wide range of biological activities in bacteria,  
55 fungi, plants, and mammals (Molina-Torres *et al.* 1996; Gertsch, 2008; Prachayasittukul *et*  
56 *al.* 2013). These include antimicrobial and other activities that suggest these compounds may  
57 function in defence against competing plants, microbes, and herbivorous pests (Molina-  
58 Torres *et al.* 2004) Affinin (*N*-isobutyl-2*E*,6*Z*,8*E*-decatrienamide) is the most abundant  
59 alkamide found in the ethanolic root extracts from chilcuague [*Heliopsis longipes* (A. Gray)  
60 S. F. Blake], an endemic species from “Sierra Gorda”, México. This molecule has been  
61 shown to have bacteriostatic and fungistatic effects (Molina-Torres *et al.* 1996) and to alter  
62 plant root growth and development (Ramírez-Chávez *et al.* 2004). More detailed plant  
63 developmental studies have found that alkamides also alter signalling in plants, modulating  
64 both developmental and stress response pathways, functioning as biochemical elicitors  
65 (López-Bucio *et al.* 2007; Méndez-Bravo *et al.* 2011). Most organisms contain amide lipids  
66 composed of one or two amines linked to a fatty acid through an amide bond in their inner  
67 and outer membranes. *N*-acylethanolamides (NAEs), which include some endocannabinoids,  
68 are an example of amine lipids structurally related to alkamides that have important  
69 biological signalling functions in plants (Blancaflor *et al.* 2003; Coulon *et al.* 2012;  
70 Blancaflor *et al.* 2014) and in mammals (Kunos *et al.* 2000; Wilson and Nicoll, 2002). Faure  
71 *et al.* (2014) found that alkamides could alter the NAE metabolic pathway by modulating  
72 fatty acid amide hydrolase (FAAH) activity. However, they also concluded that metabolic  
73 pathways other than FAAH are also involved in the metabolism of alkamides in plants,  
74 indicating the need for further studies in this area. Alkamides also exhibit structural  
75 similarities to *N*-acyl-homoserine lactones (AHLs), another amino lipid compound used by  
76 many bacteria as quorum-sensing signals to coordinate their collective behaviour.  
77 Accumulating evidence indicates that AHL are also perceived by plants, which respond by  
78 altering cell immune responses, host defence, stress responses, energy and metabolic

79 activities, transcriptional regulation, protein processing, cytoskeletal activities, root  
80 development and plant hormone responses (Mathesius et al. 2003; Kravchenko et al. 2006).

81 Affinin isolated from *Heliopsis longipes* roots displays a dramatic effect on *Arabidopsis*  
82 *thaliana* (*Arabidopsis*) root system architecture by altering primary root growth, lateral root  
83 emergence, and increasing root hair elongation in a dose dependent manner (Ramírez-Chávez  
84 *et al.* 2004). Méndez-Bravo *et al.* (2010) found that *N*-isobutyl decanamide and the  
85 interacting signals JA and nitric oxide (NO) act downstream independently of auxin-  
86 responsive gene expression to promote lateral root formation and emergence, providing  
87 compelling evidence that NO is an intermediate in alkamide signalling mediating the root  
88 system architecture alterations observed in *Arabidopsis*. Transcriptomic profiling of  
89 *Arabidopsis* has shown that exogenous application of *N*-isobutyl decanamide triggers  
90 profound physiological changes with activation of developmental, defence, and stress related  
91 genes (Mendez-Bravo *et al.* 2011). Transcripts of several JA-related genes such as *PDFs*,  
92 *VSP2*, *JAZ10* and *JAZ8* accumulated to higher levels. Transcripts of at least 70 genes  
93 belonging to the functional group “oxygen and radical detoxification”, also exhibited  
94 enhanced accumulation by *N*-isobutyl decanamide treatment. They found that alkamides  
95 could modulate some - defence responses associated with necrotrophic pathogens through  
96 JA-dependent and MPK6-regulated signalling pathways. Additionally, decanamide induces  
97 ROS accumulation in leaf tissue (Mendez-Bravo *et al.* 2011). These results suggest that  
98 general defence-associated responses elicited by *N*-isobutyl decanamide and affinin appear  
99 to be related to both hormone and ROS signalling pathways.

100 Recent studies revealed that ROS act as essential signalling molecules in plants and are  
101 required for several basic biological processes including cellular proliferation and  
102 differentiation, immunity, and stress responses (Mittler, 2017). ROS signalling specificity is  
103 dependent on the species produced and their subcellular location. It is well known that ROS,  
104 such as superoxide anion ( $O_2^{\cdot-}$ ), hydrogen peroxide ( $H_2O_2$ ), hydroxyl radical ( $\cdot OH$ ), and  
105 singlet oxygen ( $^1O_2$ ), play important signalling roles in plants as key regulators of growth,  
106 development, response to biotic and environmental stimuli, plant metabolism, and  
107 programmed cell death (Jaspers and Kangasjärvi, 2010; Suzuki *et al.*, 2011; del Río, 2015;  
108 Overmyer *et al.*, 2003). In plants,  $H_2O_2$  is the product of catalytic reactions from different

109 enzymes such as the peroxisomal flavin-containing enzymes glycolate oxidase and the acyl-  
110 CoA oxidase, which are involved in the photorespiratory and fatty acid  $\beta$ -oxidation pathways,  
111 respectively.  $H_2O_2$  is produced in the chloroplast under normal and stress conditions, as well  
112 as from the activities of peroxidases, and in some species, oxalate oxidase (Torres, 2010;  
113 Baxter et al., 2014). It is now well established that a major source of the  $O_2^{\cdot-}$  is the plasma  
114 membrane-localized NADPH-oxidases (del Río, 2015).  $O_2^{\cdot-}$  is a charged molecule under most  
115 physiological conditions and can not passively transfer across a membrane. However,  $O_2^{\cdot-}$   
116 can dismutate into  $H_2O_2$ , either enzymatically by superoxide dismutase (SOD), peroxidases  
117 or spontaneously, especially at low pH.  $H_2O_2$  can readily cross membranes passively or via  
118 aquaporins. Additionally,  $O_2^{\cdot-}$  can mediate the formation of membrane soluble lipid  
119 peroxides (Miller *et al.*, 2010; Mittler *et al.*, 2011). In many biological systems (as animals  
120 and plants) ROS signalling is mediated by a highly regulated process of ROS accumulation  
121 in specific cellular compartments. The NADPH-oxidases, termed *NOX* in animals and  
122 RESPIRATORY BURST OXIDASE HOMOLOGs (RBOHs) in plants, are plasma  
123 membrane localized enzymes that produce ROS into the apoplast. This family of enzymes  
124 are highly regulated via calcium and various phosphorylation/dephosphorylation events  
125 (Ogasawara *et al.* 2008; Mittler, 2017). In *Arabidopsis* the ROS produced by the NADPH-  
126 oxidases RBOHC, RBOHD, and RBOHF, as well as the class III peroxidases, have been  
127 shown to be involved in the lateral root emergence and root hair growth (Ogasawara *et al.*  
128 2008; Li *et al.* 2015; Orman-Ligeza *et al.* 2016; Manzano *et al.* 2014, Fernández-Marcos *et*  
129 *al.* 2017). Nevertheless, the source of alkamide-induced ROS production and the signalling  
130 pathways recruited downstream that lead to modifications in root growth, development, and  
131 plant metabolism remain unknown. Here we utilize a genetic approach to address the role of  
132 ROS signalling in alkamide-induced processes.

## 133 **Materials and Methods**

### 134 **Plant material and growth conditions.**

135 *Arabidopsis thaliana* (*Arabidopsis*) accession Columbia-0 (Col-0) was used for all  
136 experiments unless otherwise indicated. For reverse genetic experiments, the following  
137 mutants were used; the NADPH-oxidases, *respiratory burst oxidase homologC* (*rbohC*),

138 *rbohD*, and *rbohF*; class III peroxidase, *peroxidase34* (*prx34*); heterotrimeric G-protein  
139 subunits, *g-protein alpha subunit1-2* (*gpa1-2*), *arabidopsis gtp-binding protein beta1-2*  
140 (*agb1-2*), *arabidopsis g-protein gamma subunit2-1* (*agg2-1*), and the *regulator of g-protein*  
141 *signaling1-2* (*rgs1-2*). Mutant seeds were obtained from NASC ([www.arabidopsis.info](http://www.arabidopsis.info)).  
142 Seeds were surface sterilized with 70% (v/v) ethanol plus 2% triton-X 100 for 5 min, then  
143 rinsed in absolute ethanol for 1 min, and dried in a laminar hood over sterile filter paper  
144 sheets. Seeds were germinated and grown on agar plates (9 g L<sup>-1</sup>) containing 0.3x MS  
145 medium and sucrose (11 g L<sup>-1</sup>). Seeds were stratified 72 hrs in darkness at 4°C and then  
146 placed in controlled environment growth chambers (Weiss FITOTRON SCG120;  
147 [www.fitotron.co.uk](http://www.fitotron.co.uk)) vertically to allow root growth along the agar surface and unimpeded  
148 hypocotyl growth. Plants were grown under a long-day photoperiod (16 h light, 8 h darkness),  
149 25°C/18°C day/night temperature and a light intensity of 60-100 μM m<sup>-2</sup> s<sup>-1</sup>. After  
150 germination for four days, seedlings were transferred to plates containing solvent control or  
151 affinin treatments (10 or 50 μM). For the pharmacological assay, one-week old seedlings  
152 were transferred to a solid medium supplemented individually or in various combinations of  
153 affinin (7 or 50 μM), diphenyleneiododum (DPI; 0.3μM), and solvent control for seven days.  
154 In MES buffer experiments, four-day-old seedlings were transferred to medium  
155 supplemented with MES buffer (0.5g L<sup>-1</sup>); after the addition of all the reagents the pH was  
156 adjusted to 5.7 with NaOH and then autoclaved. After autoclaving, treatments were  
157 prepared adding the affinin (10 or 50 μM) to the medium. After seven days the primary root  
158 length, number of emerged lateral roots and root hair length were evaluated.

### 159 **Affinin isolation and purification.**

160 Affinin extraction was performed as previously reported by Ramírez-Chavez *et al.* (2004).  
161 After extraction, the concentrated oil was weighted, 2 g were purified by column  
162 chromatography as previously reported by Ramírez-Chávez *et al.* (2004); subsequently, the  
163 purified fraction was analysed by GC/EIMS to confirm its purity and concentration.

### 164 **ROS staining.**

165 H<sub>2</sub>O<sub>2</sub> accumulation was monitored *in situ* with 3,3'-diaminobenzidine tetrachloride (DAB;  
166 Sigma-Aldrich; [www.sigmaaldrich.com](http://www.sigmaaldrich.com)) based on the method of (Thordal-Christensen *et al.*,

167 1997). Six-day-old seedlings were immersed in DAB (1 mg ml<sup>-1</sup>) in PBS buffer (10 mM; pH  
168 7.0) plus 0.05% (v/v) tween-20 and placed overnight at room temperature in the dark. O<sub>2</sub><sup>•-</sup>  
169 was detected based on nitroblue tetrazolium (NBT)-reducing activity. Seedlings were  
170 covered in an NBT solution (0.5mg ml<sup>-1</sup>) in 0.1M PBS buffer (pH 7.4) plus 0.05% triton-X  
171 100 and incubated in the light for 10 minutes. DAB and NBT reactions were stopped by  
172 replacing staining solution with fixative / clearing solution of ethanol / acetic acid / glycerol  
173 (3:1:1) for 24 hours, mounted on glass slides with a coverslip and visualized with a Leica  
174 2500 microscope ([www.leica-microsystems.com](http://www.leica-microsystems.com)).

### 175 **Root growth analysis and microscopy.**

176 Root growth measurements were performed on images taken from the plates using the  
177 SmartRoot plugin on ImageJ ([www.imagej.net](http://www.imagej.net); <https://smartroot.github.io/>). For the analysis  
178 of emerged lateral roots, root samples were visualized with a Leica MZ10F stereo microscope  
179 equipped with a model DFC490 digital camera attachment (Leica; [www.leica-](http://www.leica-microsystems.com)  
180 [microsystems.com](http://www.leica-microsystems.com)) and lateral roots protruding beyond the epidermal tissue were scored as  
181 emerged. Primary root zone organisation of seedlings with or without 50µM affinin treatment  
182 were visualised with 5 mg/ml propidium iodide stain and observed in a Carl Zeiss LSM800  
183 confocal laser microscope (<https://www.zeiss.com/>). Measurements of distance from primary  
184 root tip to first root hair bulge, cell length from the elongation/differentiation zone (EZ/DZ)  
185 and apical meristem length (AM) were made with ImageJ software ([www.imagej.net](http://www.imagej.net)). DAB  
186 staining images were taken with a Leica 2500 microscope with differential interference  
187 contrast (DIC) optics (<https://www.leica-microsystems.com/>). For each treatment, at least ten  
188 plants were analysed. Representative plants for each treatment were photographed using the  
189 Nomarski optics on a Leica 2500 microscope. Quantification of DAB staining intensity was  
190 done by ImageJ-based quantification described by Béziat (2017). Prior to quantification, the  
191 colour mode of light micrographs was converted from RGB to HSB by using ImageJ software  
192 and the saturation channel in the HSB stack was selected. Then the intensity of DAB staining  
193 was measured in the saturation channel from a same size area in all pictures. An increase of  
194 saturation depicts more “pure” colour, while a decrease denotes a more “washed-out” signal  
195 (Béziat *et al.*, 2017).



196 **Bromocresol purple pH assay.**

197 To test pH changes in the roots, seven-day-old *Arabidopsis* seedlings Col-0 were transferred  
198 to a solid medium (as described before) with different affinin treatments. At 24 hours,  
199 seedlings were transferred from treatments to a glass slides covered with 1ml of the pH  
200 indicator bromocresol purple ([www.sigmaaldrich.com](http://www.sigmaaldrich.com); 0.04 g L<sup>-1</sup>) in agarose (0.7%)  
201 prepared with distilled water plus CaSO<sub>4</sub> (0.2mM) (Zandonadi *et al.*, 2010). The pH was  
202 adjusted to 7.5 with NaOH. After 30 min, glass slides with the seedlings were photographed  
203 with a CAMAG TLC Visualizer ([www.camag.com](http://www.camag.com)). Photographs were analysed with  
204 ImageJ software as follows. First, images were converted to an 8-bit format and calibrated  
205 with a set of density standards (pH scale bar), a region of interest (ROI) was selected from  
206 each pH scale point and the mean grey value of each of those points was recorded and then  
207 fitted to a “curve fitting method (linear function)” from the popup menu as described in the  
208 ImageJ user manual (<https://imagej.nih.gov>).

209 **Statistical analysis.**

210 Data from mutant sets were analysed with two-way ANOVA ( $n = 10$ ) and a Tukey’s posthoc  
211 test using the Minitab 14 software ([www.minitab.com](http://www.minitab.com)). Different letters are used to indicate  
212 significance groups (means that differed significantly  $P \leq 0.05$ ). For single genotype  
213 experiments, data were analysed with one-way ANOVA ( $n = 10$ ) and Tukey’s posthoc test  
214 ( $P \leq 0.05$ ) using InfoStat software ([www.infostat.com.ar](http://www.infostat.com.ar)).

215

216 **Results**

217 **Root phenotype of *Arabidopsis Col-0* in response to affinin.**

218 To establish the principal affinin-induced phenotypes in seedlings of WT Col-0 *Arabidopsis*  
219 under our conditions, root architecture was monitored in response to two affinin  
220 concentrations (10  $\mu$ M and 50  $\mu$ M), in aseptic cultures on 0.3x MS solid medium. After seven  
221 days of growth, the 10  $\mu$ M treatment resulted in an increased number of emerged lateral roots  
222 without a significant decrease on the primary root length (Fig. 1A-C). The 50  $\mu$ M treatment



223 reduced growth monitored as primary root length and resulted in a significantly increased  
224 number of emerged lateral roots and root hair length (Fig. 1A-D). These results show that  
225 affinin treatments influenced *Arabidopsis* root system architecture, consistent with the  
226 previously reported phenotypes induced by affinin and decanamide (Ramírez-Chávez *et al.*,  
227 2004; López-Bucio *et al.*, 2007; Méndez-Bravo *et al.*, 2010; Méndez-Bravo *et al.*, 2011).

### 228 **Affinin alters H<sub>2</sub>O<sub>2</sub> accumulation in root meristems and lateral root emergence sites.**

229 *Arabidopsis* transcriptional signatures (Méndez-Bravo *et al.* 2011) suggest that *N*-isobutyl  
230 decanamide modulates ROS signalling, which is involved in root development (Passardi *et*  
231 *al.* 2006; Manzano *et al.* 2014), prompting us to assay for affinin-induced ROS responses in  
232 *Arabidopsis* roots. DAB staining was utilized to visualize affinin-induced changes in H<sub>2</sub>O<sub>2</sub>  
233 accumulation *in situ*. Staining with DAB forms a brown-reddish precipitate in the presence  
234 of H<sub>2</sub>O<sub>2</sub> and peroxidase activity. In the root meristematic zone, the deposition of DAB stain  
235 was reduced by treatment with 50 μM affinin, but no change in DAB staining was seen in  
236 the elongation or maturation zones (Fig. 2A). O<sub>2</sub><sup>•-</sup> accumulation detected by NBT staining  
237 remained unchanged (Fig. 2B). DAB staining was significantly higher in the lateral root  
238 primordia emergence sites of roots treated with 50 μM affinin but reduced in the apical  
239 meristem (Fig. 2A-F). These results suggest that H<sub>2</sub>O<sub>2</sub> is involved in affinin-induced changes  
240 in lateral root emergence and root apical meristem development leading to an increase in  
241 emerged lateral roots and a reduction of primary root length in response to the affinin  
242 treatments. These results demonstrate a correlation between sites of H<sub>2</sub>O<sub>2</sub> accumulation and  
243 developmental responses to affinin, prompting further exploration of the role of ROS in these  
244 processes.

### 245 **Affinin-induced *Arabidopsis* lateral rooting is dependent of endogenous H<sub>2</sub>O<sub>2</sub>.**

246 To test ROS involvement in affinin-induced changes in root architecture, a pharmacological  
247 approach was first employed. The effects of affinin on root development were tested in the  
248 presence of diphenyleneiododum (DPI), a NADPH oxidase inhibitor. Plants grown in  
249 medium containing DPI plus affinin did not show the characteristic affinin induced  
250 phenotypes (Fig. 2E). Specifically, seedlings grown on DPI did not increase the number of  
251 lateral roots in the presence of affinin; the number of lateral roots in these seedlings remained

252 the same as it was prior to being transferred. Affinin at 7  $\mu$ M increased the primary root  
253 length a response reported by Ramírez-Chávez *et al.* (2004), in contrast primary root growth  
254 was totally inhibited by DPI (Fig. 2H-I). These results suggest that endogenous ROS is  
255 required for affinin-induced lateral root growth and for primary root development, prompting  
256 us to use reverse genetics to define the sources of ROS that are involved in mediating these  
257 root architecture changes.

### 258 **PRX34-mediated H<sub>2</sub>O<sub>2</sub> production in affinin-induced responses.**

259 The cell wall associated class III peroxidases (PRXs) have been implicated in lateral root  
260 formation and regulation of root tip growth (Passardi *et al.* 2006; Manzano *et al.* 2014). The  
261 *prx34* mutant (Bindschedler *et al.*, 2006) was assayed for affinin-induced root structure  
262 alterations and associated DAB stain accumulation. The *prx34* mutant exhibited enhanced  
263 inhibition of primary root growth in response to high affinin concentration (Fig. 3A), which  
264 was associated with a drop in DAB staining intensity in the meristematic zone (Fig. 3C, D),  
265 suggesting that modulation of ROS signalling by PRX34 is implicated in the regulation of  
266 meristematic processes by affinin. The number of emerged lateral roots in *prx34* was not  
267 increased by affinin treatment (Fig. 3B), while the enhanced DAB staining seen in affinin  
268 treated wild type Col-0 plants was not observed in the lateral root emergence sites of *prx34*  
269 roots (Fig. 3C, D). These results support that PRX34 was required for alkamide-induced  
270 signalling leading to lateral root emergence and suggest that the ROS produced or modulated  
271 by PRX34 is involved in this process.

### 272 **NADPH-oxidase mediated ROS production in affinin-induced developmental changes.**

273 We next sought to further define the sources of affinin-induced ROS. To explore the  
274 contribution of ROS signalling from the RBOH NADPH oxidases in responses to affinin, the  
275 root system architecture of wild type plants and the *rbohC*, *rbohD*, and *rbohF* single mutants  
276 were compared following growth in the presence of different affinin concentrations. In  
277 medium lacking affinin, all *rboh* mutants exhibited reduced primary root growth as compared  
278 to wild type (Fig. 4A) and reduced DAB stain deposition was apparent in the root tips of  
279 *rbohC* and *rbohD*, but not *rbohF* under control conditions (Fig. 4C). Primary roots treated  
280 with affinin in all mutants showed behaviour similar to WT, however, the *rbohC*, *rbohD*, and

281 *rbohF* mutants had enhanced growth inhibition at 50 $\mu$ M affinin (Fig. 4A). DAB staining of  
282 the apical meristems (Fig. 4C) showed that affinin at 50  $\mu$ M reduced the H<sub>2</sub>O<sub>2</sub> accumulation  
283 in WT, *rbohC* and *rbohD* but no decrease was observed in *rbohF* (Fig. 4C,E). These results  
284 suggest that primary root growth inhibition caused by affinin could be mediated via  
285 attenuation of ROS accumulation sourced from RBOHC and RBOHD, but not RBOHF. The  
286 *rbohC* and *rbohD* mutants lacked a significant affinin-induced increase in emerged lateral  
287 root number (Fig. 4B). DAB staining at lateral roots emergence sites was not enhanced in  
288 both mutants (*rbohC* and *rbohD*) treated with 50  $\mu$ M affinin while in *rbohF* staining was  
289 higher in response to 50  $\mu$ M affinin (Fig. 4D, F) suggesting that RBOHC and RBOHD could  
290 be involved in promotion of lateral root emergence via alkamide-induced ROS accumulation.

291 ROS produced by RBOHC is required for cell expansion in root hair growth and  
292 characteristically the *rbohC* mutant has greatly reduced root hair length (Foreman *et al.*  
293 2003). Intriguingly, root hair length was unchanged upon affinin-treatment of the *rbohC*  
294 mutant indicating that ROS produced by this NADPH-oxidase is necessary for affinin-  
295 induced enhanced root hair expansion (Fig. 4G, H). The *rbohD* and *rbohF* mutants had  
296 significantly longer root hairs under affinin-treatment (Fig. 4G, H) suggesting that these ROS  
297 sources had a minor role as negative regulators of this process. These results highlight the  
298 importance of *RBOHC*-mediated ROS production for enhanced root hair expansion.

### 299 **G-protein signalling in the *Arabidopsis* affinin response.**

300 To test if the heterotrimeric (ht) G-protein subunits, G $\alpha$ , G $\beta$  and G $\gamma$ , are involved in  
301 *Arabidopsis* response to affinin, affinin-induced root phenotypes of *gpa1-2*, *agb1-2*, and  
302 *agg2-1* mutant plants were examined. In all genotypes primary root length was reduced by  
303 50  $\mu$ M affinin treatments and in *agb1-2* this effect was slightly but significantly enhanced  
304 suggesting AGB2 may act as a negative regulator of this process (Fig. 5A). The *agb1-2* and  
305 *agg2-1* mutants exhibited and increased number of lateral roots under control conditions,  
306 indicating that they negatively regulate lateral root formation (Fig. 5B). Interestingly, *agb1-*  
307 *2* exhibited a decrease in the number of lateral roots under affinin treatment compared to  
308 control (0 $\mu$ M affinin), while *agg2-2* remained equal in affinin treatment and control, and  
309 *gpa1-2* had a slight but not significant increase, suggesting that all these subunits could be

310 required for enhanced lateral root emergence in response to affinin (Fig.5B). In plants  $G_{\alpha}$   
311 proteins tend toward their active GTP bound state (Urano and Jones, 2014) and the seven  
312 transmembrane domains (7TMD) containing RGS1 protein negatively regulates GPA1-  
313 mediated signalling through its GTPase accelerating protein (GAP) activity (Liang *et al.*  
314 2018). The *rgs1-2* mutant was also tested and had a reduced primary root length under control  
315 conditions (Fig. 5C) indicating RGS2 is required for full primary root growth. Affinin  
316 treatment reduced primary root length to a similar extent in both Col-0 WT and *rgs1-2* (Fig.  
317 5C) suggesting RGS1 is not involved in affinin-induced response on primary root growth.  
318 Lateral root emergence was the same in WT and *rgs1-2* under control conditions, but the  
319 affinin-induced increase was enhanced in *rgs1-2*, suggesting RGS1 negatively regulates this  
320 response (Fig. 5D). Together, these data implicate multiple htG-protein subunits in the  
321 regulation of the affinin response.

## 322 **Extracellular pH and affinin-induced responses.**

323 To test if affinin causes changes in apoplastic pH, an affinin pulse for 24 hours (see Materials  
324 and Methods) was applied to seven-day-old *Arabidopsis* roots and changes in the pH in  
325 surrounding growth medium was monitored with the indicator bromocresol purple. The  
326 results show that affinin treatment induced extracellular acidification in the root elongation  
327 zone (Fig. 6A, B). To test the potential functional consequence of these extracellular pH  
328 changes, the extracellular pH was stabilized using a medium containing 2-(*N*-morpholino)  
329 ethanesulfonic acid (MES) buffer (pH 5.7), which has an active buffering capacity in the  
330 relevant range of pH 5.5 - 6.7. In buffered medium, affinin treatment exhibited typical  
331 inhibition of primary root growth; however, the number of emerged lateral roots did not  
332 increase in response to affinin (Fig. 6C-E). Further, in line with previous studies (Kagenishi  
333 *et al.* 2016), root hair growth was inhibited in control plants on buffered medium without  
334 affinin; however, root hair length still increased upon affinin treatment on MES buffered  
335 medium (Fig. 6F, G). We conclude that the affinin-induced changes in lateral root emergence,  
336 but not root hair length, were dependent on a change in extracellular pH.

## 337 **Discussion**

### 338 **The role of ROS in alkamide-induced processes.**

339 Decanamide-induced transcriptional reprogramming previously observed in *Arabidopsis*  
340 (Mendez-Bravo et al. 2011) suggests ROS signalling may mediate alkamide-induced  
341 processes. The current study utilizes a genetic approach with the previously established  
342 model system (Ramírez-Chávez et al. 2004; Méndez-Bravo et al. 2010) of alkamide-induced  
343 alterations to *Arabidopsis* root system architecture to demonstrate that these developmental  
344 changes are associated with changes in ROS accumulation, as monitored using NBT to  
345 visualize  $O_2^{\bullet-}$  production and DAB for  $H_2O_2$  (Figs. 2-4). Additionally, this study builds upon  
346 the previous observation of affinin-induced  $H_2O_2$  accumulation in *Arabidopsis* leaves  
347 (Méndez-Bravo et al. 2011) by expanding findings to root tissues undergoing developmental  
348 changes. We found that 50  $\mu$ M affinin induced the accumulation of  $H_2O_2$  in the peripheral  
349 cells surrounding the lateral root primordia (Fig. 2C, D), which coincided with an increased  
350 number of emerged lateral roots (Fig. 1A, B). These data are consistent with the known  
351 signalling role of  $H_2O_2$  in lateral root development as previously reported (Passardi et al.  
352 2006; Manzano et al. 2014; Tsukagoshi et al. 2016; Orman-Ligeza et al. 2016) and suggest  
353 that  $H_2O_2$  is involved in root response to alkamides by acting as a signalling intermediate.  
354 Further, these results are consistent with the ability of ROS to increase lateral root numbers  
355 due to the activation of lateral root pre-branch sites and lateral root primordia. Specifically,  
356 ROS are deposited in the apoplast of these cells during lateral root emergence (Orman-Ligeza  
357 et al. 2016).

358 Moreover, our results indicate that affinin attenuated growth of the primary root in a dose  
359 dependent manner (Fig. 1A, C), which was accompanied by attenuated DAB staining  
360 intensity specifically in the root meristematic region (Fig. 2A, C, D). Root growth is  
361 controlled by both the rate of cell division in the meristematic zone and the degree of cell  
362 expansion in the elongation zone (Beemster and Baskin, 1998; Tsukagoshi et al. 2010).  
363 Increased root meristem size is correlated with an acceleration of root growth and is a result  
364 of increased rates of cell division and the delay of cell expansion (Ubeda-Tomas et al. 2009;  
365 Tsukagoshi et al. 2010). It has been demonstrated that  $H_2O_2$  and the  $O_2^{\bullet-}$  both have distinct  
366 accumulation zones and distinct roles in the growing *Arabidopsis* root (Dunand et al. 2007).  
367 Our results demonstrate that affinin altered the accumulation of  $H_2O_2$ , but not  $O_2^{\bullet-}$ , in the  
368 meristem (Fig. 2A, B). Affinin treatment reduced the cell size of the root elongation-  
369 differentiation zone (Fig. 1E-M) without altering  $H_2O_2$  and  $O_2^{\bullet-}$  accumulation in this root

370 zone (Fig. 2A, B) indicating that affinin can modulate a defined developmental program.  
371 This profile of changes is consistent with the action of peroxidases, which are known to  
372 modulate primary root growth (Passardi *et al.* 2006). These results agree with the findings  
373 that affinin alter meristematic root growth and the expression of *CycB1* gene (Ramírez-  
374 Chávez *et al.*, 2004).

375 We also present evidence supporting the involvement of extracellular acidification in  
376 response to affinin. Ion fluxes are a common event that often works in concert with ROS  
377 signalling in stress and developmental responses. It is known that changes in apoplastic pH  
378 are likely to modulate the activity of several regulatory elements such as cell wall proteins,  
379 such as expansins (Cosgrove *et al.* 2002) and pectin methylesterases (Sherrier and  
380 Vandenbasch, 1994, Micheli, 2001); plasma membrane proteins, such as pH-sensitive  
381 potassium channels (Ilan *et al.* 1996, Hartje *et al.* 2001); and is functionally related with the  
382 regulation of root hair growth (Monshausen *et al.* 2007).

383 Beyond correlating ROS accumulation with affinin-induced changes in root system  
384 architecture, pharmacological treatments and mutant plants with compromised ROS  
385 pathways (Figs. 3-5) were utilized to reveal a requirement for these ROS-signalling pathways  
386 for a subset of affinin-induced developmental responses. Based on this pharmacological and  
387 genetic evidence, we conclude that ROS-signalling was involved in affinin-induced  
388 responses. This work also defined the sources of various affinin-responses, as further  
389 discussed below.

390 The production of ROS in the apoplast depends on several classes of enzymes, most notably,  
391 NADPH-oxidases and class III peroxidases. Several NADPH-oxidases are known ROS  
392 sources that mediate cell expansion and determines root system architecture (Torres, 2010).  
393 These are known in *Arabidopsis* as RESPIRATORY BURST OXIDASE HOMOLOGS  
394 (RBOHs) and act specifically in lateral root emergence, and root hair cell expansion  
395 (Foreman *et al.* 2003; Orman-Ligeza *et al.* 2016), while class III peroxidases, such as  
396 *AtPrx34*, have been associated with an active role in root cell elongation (Sagi and Fluhr,  
397 2006; Passardi *et al.*, 2006).



398 To test if these ROS sources are involved in affinin-response, several available *Arabidopsis*  
399 mutants were utilized, including *prx34*, which is defective in a class III peroxidase, and the  
400 NADPH-oxidase mutants, *rbohC*, *rbohD*, and *rbohF*. Testing the effect of affinin in the  
401 *prx34* mutant, the ROS staining pattern of lateral root primordia and the number of emerged  
402 lateral roots were indistinguishable from wild type Col-0 plants (Fig. 3C, D). It has been  
403 demonstrated that *PRX* activities are important for lateral root development, especially during  
404 lateral root emergence (Manzano *et al.*, 2014). The effects of affinin on root system  
405 architecture has been previously shown to be independent or downstream of auxin signalling  
406 (Méndez-Bravo *et al.*, 2010). Accordingly, lateral root emergence due to *PRX* activity also  
407 occurs independent of auxin signalling (Manzano *et al.* 2014). The accumulation of DAB  
408 staining in root tips was reduced by affinin 50  $\mu$ M in *prx34* as in WT. It has been reported  
409 that peroxidases are involved in the regulation of primary root growth (Tsukagoshi *et al.*  
410 2010) and *PRX34* was previously shown to be required as a component of the oxidative burst  
411 in response to some pathogens (Bindschedler *et al.*, 2006). Our results strongly suggest that  
412 *PRX34* is not required for affinin-induced inhibition of primary root growth, suggesting other  
413 *PRXs* may regulate this process. The reduced accumulation of DAB staining in root  
414 meristems upon 50  $\mu$ M affinin treatment suggests that ROS homeostasis is somehow  
415 disrupted due to affinin treatment leading to an alteration in plant cell cycle. This result is  
416 supported by the fact that affinin at high concentrations reduced the expression of genes  
417 associated with the mitotic cycle, such as *CycB1* (Ramírez-Chávez *et al.*, 2004). On this topic,  
418 it has been found that cellular ROS signalling oscillations are rapidly transmitted through  
419 MAPK pathways inducing MAP activation and affects microtubules dynamics and  
420 organization (Livanos *et al.*, 2012).

421 Using the *respiratory burst oxidase homologues (RBOH)* mutants (*rbohC*, *rbohD* and *rbohF*)  
422 these ROS signalling genes were tested for involvement in alkamide induced signalling. This  
423 revealed that primary root growth inhibition by affinin was independent of all the loci  
424 represented by these mutant lines (Fig.4A), however H<sub>2</sub>O<sub>2</sub> accumulation as monitored by  
425 DAB staining in the apical meristem was reduced in the *rbohC* and *rbohD* mutants while  
426 unchanged in *rbohF* (Fig. 4C, E). Interestingly the *rbohD* mutant exhibited a significant  
427 inhibition of primary root length in response to affinin compared to the other two mutants  
428 and wild type. Taken together, the primary root length and DAB staining results do not



429 support that the ROS produced by *rbohC* and *rbohF* are involved in affinin-induced response  
430 in meristematic activity. However, the impact of affinin on root length in *rbohD* supports the  
431 hypothesis that ROS homeostasis could be involved in mediating affinin response in  
432 meristematic cells. On the other hand, *rbohC* and *rbohD* failed to increase the number of  
433 emerged lateral roots in response to affinin (Fig. 4B) and the DAB staining intensity did not  
434 show differences in lateral root primordia between the treatments of these mutants (Fig. 4D,  
435 F). These results are consistent with Orman-Ligeza *et al.* (2016), who found that *RBOH*-  
436 mediated ROS production facilitates lateral root outgrowth by promoting cell wall  
437 remodelling of overlying parental tissues. Indeed, the diverse transcription patterns suggest  
438 that *RBOHs* function in broad aspects of growth and physiological response (Sagi and Fluhr,  
439 2006). In contrast, *rbohF* response in terms of emerged lateral roots was similar to the wild  
440 type of response induced by affinin and the DAB staining showed similar results (Fig. 4D,  
441 F).

442 The effect of affinin on root hair growth has been demonstrated (Ramírez-Chávez, *et al.*  
443 2004) and corroborated (Fig. 4G). Interestingly, *rbohC* was the only mutant that did not  
444 respond to affinin-induced enhanced root hair elongation (Fig. 4G), this result not only  
445 demonstrates the importance of ROS in affinin induced signalling but also the specificity of  
446 ROS produced by *RBOHC* on root hair growth. The *rbohD* and *rbohF* mutants exhibited an  
447 increase in root hair length higher than the wild type seedlings (Fig.4G), which indicates that  
448 these ROS sources could be negative regulators of root hair growth.

449 In ROS metabolomic studies, the “oxidative stress” signature includes accumulation of  
450 several compounds implicated in ascorbate and glutathione synthesis and degradation  
451 pathways, and phytohormones such salicylic acid and jasmonic acid (Noctor *et al.*, 2016).  
452 Additionally, this signature also includes several compounds whose connections to  
453 antioxidant metabolism and redox homeostasis are not as obvious. For example, the  
454 accumulation of branched chain amino acids induced by ABA treatment, a response that  
455 seems to occur reproducibly during redox signalling (Ghassemian *et al.*, 2008; Noctor *et al.*,  
456 2015). Recently in tomato seedlings it was found that, affinin induced a dose-dependent  
457 metabolomic reprogramming that lead to enhanced accumulation of amino acids, organic  
458 acids, sugar alcohols, phenolics, and fatty acids (Campos-García and Molina-Torres, 2021),

459 all metabolites that have been associated with marker metabolites in the oxidative stress  
460 response.

#### 461 **The Alkamide-induced developmental program.**

462 The details concerning how alkamides affect plant growth remain poorly characterized.  
463 Exogenous application of affinin to plants has multiple effects on several plant processes,  
464 some of which are similar to responses triggered by some well-known stress related signals.  
465 Comparison of affinin-response to these other better characterized signalling pathways may  
466 offer insight into affinin-induced signalling.

467 Biotic and abiotic stresses induce the so-called stress-induced morphogenic response  
468 (SIMR), which shares some similarities with the alkamide response. NO is an intermediate  
469 in both SIMR (Potters et al., 2009) and alkamide signalling mediating alteration in root  
470 system architecture in *Arabidopsis* (Méndez-Bravo *et al.* 2010). Altered root branching,  
471 inhibition of cell elongation, as well as changes in apoplastic pH, ROS, and redox signalling,  
472 are all common to alkamide-response and SIMR (Potters et al., 2007, Potters et al., 2009;  
473 Tongnetti et al., 2012) It is possible that alkamide-induced stress results in SIMR. However,  
474 auxin features prominently in the regulation of SIMR and it was demonstrated that alkamides  
475 act via an auxin-independent signalling pathway (Ramírez-Chávez *et al.* 2004). Nonetheless,  
476 the possibility that some alkamide-induced responses are related to SIMR may be worth  
477 further consideration.

478 Although auxins are considered the major plant growth-regulating hormones underlying root  
479 system architecture adjustment, the discovery of novel signal molecules such as *N*-acyl  
480 amides, *N*-acyl ethanolamides (NAE) and *N*-acyl homoserine lactones (AHLs) has shed light  
481 on the intricate signalling networks that trigger root system architecture modifications and  
482 physiological responses (Ramírez-Chávez *et al.*, 2004; Méndez-Bravo *et al.*, 2010; Coulon  
483 *et al.*, 2012; Schikora *et al.*, 2016). It has been demonstrated that NAEs and AHLs,  
484 compounds that are structurally related to alkamides, have a wide range of effects in plant  
485 development (Table 1), some of which overlap with affinin-induced responses. Under *in vitro*  
486 conditions, affinin shows a trend towards increasing FAAH's capacity to metabolize NAE  
487 12:0, suggesting that affinin may have some effects on plants acting via this modulation of

488 NAE metabolism. The structural similarity of affinin to NAEs, suggests that affinin might  
489 directly influence FAAH activity in plants, but this will also require further investigation  
490 (Faure *et al.*, 2015). Recently, Aziz and Chapman (2020) proposed the hypothesis that FAAH  
491 proteins hydrolyse a broader range of lipophilic substrates than previously recognized,  
492 including affinin, and consequently play a pivotal role in *N*-acyl amide-mediated plant–  
493 microbe interactions, a function beyond the established role for FAAH in seedling  
494 development in *Arabidopsis*.

495 In mammals, polyunsaturated NAEs bind to specific 7TMD G-protein coupled receptors  
496 (GPCRs) and activate the htG-proteins that regulate multiple downstream signalling  
497 pathways (Abadji *et al.*, 1999; Bosier *et al.*, 2010). In plants, htG-protein signalling has been  
498 implicated in many processes such as plant growth and development. Plant htG-protein  
499 signalling is fundamentally different from mammalian systems; with no canonical 7TMD  
500 GPCRs, the presence of novel EXTRA-LARGE G-PROTEINs (XLG1, XLG2, and XLG3),  
501 and a single G $\alpha$  subunit that has a low intrinsic GTPase activity and is self-activating in the  
502 absence of the GEF activity of GPCRs, thus tends toward a constitutively activated state  
503 (Urano *et al.*, 2016). Plant G-protein signalling has been implicated in AHL-signalling.  
504 GPA1 was required for AHL-mediated elongation of *Arabidopsis* roots (Liu *et al.*, 2012).  
505 However, we found that inhibition of primary root length by affinin was independent of  
506 GPA1.

507 In *Arabidopsis* NAE 18:3 induces stress responses, autophagy, senescence, chlorophyll  
508 catabolic genes, represses chlorophyll biosynthesis genes, and these responses require an  
509 intact htG protein complex (Yan *et al.*, 2020). Specifically, this study demonstrated the NAE  
510 18:3 response required AGB1, XLGs (using the *xlg1 xlg2 xlg3* triple mutant) and AGGs  
511 (using the *agg1 agg2 agg3* triple mutant; Yan *et al.*, 2020). The NAE 18:3 response was  
512 enhanced in the *gpa1* and *rgs1* mutants. This work also demonstrates that, due to functional  
513 redundancy in these gene families, higher order mutants are required to see clear results. Our  
514 results also showed complex profile of phenotypes with htG-protein mutants: GPA1, AGG1,  
515 and AGB1 were required for, and *rgs1* conferred hypersensitivity to affinin-induced  
516 increased lateral root emergence. For affinin-induced primary root elongation, GPA1, AGG1,  
517 and RGS1 were not required, but the *agbl* mutant conferred a slight hypersensitivity. Taken

518 together, these results suggest the similarities between affinin and NAEs warrant further  
519 exploration. Especially, further studies with additional higher order G-protein mutants will  
520 be required to resolve this question.

521 Interestingly, the *agbl-2* and *agg2-1* mutants exhibit an increased number of lateral roots  
522 under control conditions, and it is known that G $\beta\gamma$ -dimer restrains lateral root formation (Chen  
523 *et al.*, 2006). Moreover, it is reported that the *agbl* mutant has a more expanded root  
524 architecture presumably due to an increased cell proliferation and lateral root formation  
525 (Urano *et al.*, 2016). Our results show that in the *agbl-2* mutant, primary root length and  
526 lateral root number were reduced in response to affinin, which is a contrasting response  
527 compared to the mutant phenotype. Taken together these results suggest the htG-protein  
528 complex mediating plant response to affinin, modulating cell proliferation activity and lateral  
529 root emergence. Further studies will be required to clarify the mechanism involved.

## 530 **Conclusions**

531 Our results provide clear evidence that ROS are molecular intermediates involved in lateral  
532 roots emergence and root hair growth in response to alkamides. This is supported by the  
533 known roles of ROS as mediators and activators of structural changes in roots. In addition,  
534 we demonstrate that alkamides induced root extracellular pH changes, which had an effect  
535 on lateral roots emergence. These results provide us with evidence that alkamide-induced  
536 modification of root architecture depends on modifications in extracellular pH and ROS  
537 homeostasis in the lateral root emergence zone. Further, we also provided evidence that  
538 heterotrimeric G proteins can be mediating affinin-induced signalling. This is supported by  
539 evidence that some G protein subunits may be activating ROS synthesis, inducing  
540 softening of cell walls and facilitating lateral roots emergence. While, on the other hand, ROS  
541 formed specifically by RBOHC induce Ca<sup>+2</sup> channels hyperpolarization, allowing Ca entry  
542 into the cell and activating root hairs elongation. Nevertheless, further studies with additional  
543 higher order G-protein mutants will be required to resolve how htG-proteins are involved in  
544 alkamide-signaling.

545

## 546 **Acknowledgements**

547 We thank Tuomas Puukko, Airi Lamminmäki, and Leena Grönholm, for excellent technical  
548 support, Eveliina Karjalainen for assistance with mutant seed production, Dr. Huitzimengari  
549 Campos-García for help with the statistical analysis, Dr. Vincent-Cervantes Bueno for his  
550 help with the confocal microscope, and M.Sc. Enrique Ramírez-Chávez for his support in  
551 affinin purification and GC-MS analysis. The members of the Plant Stress Metagroup are  
552 acknowledged for the helpful comments and discussions during this project.

## 553 **Author Contributions**

554 Project conception and planning, TCG, KO, JM-T; experiment design, TCG, KO;  
555 experimental work, TCG; writing the manuscript, TCG, KO; editing and approval of  
556 manuscript, TCG, KO, JM-T.

## 557 **Conflicts of Interest**

558 The authors have no conflict of interest to declare. All co-authors have seen and agree with  
559 the contents of the manuscript and there is no financial interest to report. The funders had no  
560 role in the design of the study; in the collection, analyses, or interpretation of data; in the  
561 writing of the manuscript, or in the decision to publish the result.

## 562 **Funding**

563 This work was supported by the following grants: the Finnish National Agency for  
564 Education, Finnish Government Scholarship Pool (decision no. KM-18-10772) and Consejo  
565 Nacional de Ciencia y Tecnología (CONACYT) grant (426142) to TCG and the Academy of  
566 Finland Center of Excellence in the Molecular Biology of Primary Producers 2014-2019  
567 (decisions #271832 and 307335).

## 568 **Data availability**

569 The data that support the findings of this study are openly available at Campos-García *et al.*

570 (2021): Alkamides and ROS signalling. figshare. Dataset.

571 <https://doi.org/10.6084/m9.figshare.17303615.v1>.

572

## References

- Abadji, V., Lucas-Lenard, J. M., Chin, C. N., Kendall, D. A.** 1999. Involvement of the carboxyl terminus of the third intracellular loop of the cannabinoid CB1 receptor in constitutive activation of Gs. *Journal of Neurochemistry*, 72(5), 2032-2038.
- Austin-Brown, S. L., & Chapman, K. D.** 2002. Inhibition of Phospholipase D $\alpha$  by N-Acylethanolamines. *Plant Physiology*, 129(4), 1892-1898.
- Beemster GT, Baskin TI.** 1998. Analysis of cell division and elongation underlying the developmental acceleration of root growth in *Arabidopsis thaliana*. *Plant Physiology* 116,1515-1526.
- Béziat, C., Kleine-Vehn, J., & Feraru, E.** 2017. Histochemical staining of  $\beta$ -Glucuronidase and its spatial quantification. *Methods Molecular Biology* 1497, 73-80.
- Bielski BH, Allen AO.** 1977. Mechanism of the disproportionation of superoxide radicals. *The Journal of Physical Chemistry* 81(11), 1048–1050.
- Bindschedler LV, Dewdney J, Blee KA et al.** 2006. Peroxidase-dependent apoplastic oxidative burst in *Arabidopsis* required for pathogen resistance. *The Plant Journal* 47(6), 851-863.
- Blancaflor EB, Hou G, Chapman KD.** 2003. Elevated levels of N-lauroylethanolamine, an endogenous constituent of desiccated seeds, disrupt normal root development in *Arabidopsis thaliana* seedlings. *Planta* 217, 206–217.
- Blancaflor EB, Kilaru A, Keereetaweeep J, Khan BR, Faure L, Chapman KD** 2014. N-Acylethanolamines: lipid metabolites with functions in plant growth and development. *The Plant Journal* 79(4), 568-583.
- Bosier, B., Muccioli, G. G., Hermans, E., Lambert, D. M.** 2010. Functionally selective cannabinoid receptor signalling: therapeutic implications and opportunities. *Biochemical Pharmacology* 80(1), 1-12.



**Chang Y, Guo J, Gao Y, Chen JG.** 2007. Modulation of root cell division by the heterotrimeric G-proteins in Arabidopsis. *Dynamic Cell Biology* 1(1), 72-77.

**Chen, J. G., Gao, Y., Jones, A. M.** 2006. Differential roles of Arabidopsis heterotrimeric G-protein subunits in modulating cell division in roots. *Plant Physiology* 141(3), 887-897.

**Cosgrove DJ, Li LC, Cho HT, Hoffmann-Benning S, Moore RC, Blecker D.** 2002. The growing world of expansins. *Plant and Cell Physiology* 43(12), 1436–1444.

**Coulon D, Faure L, Salmon M, Wattelet V, Bessoule JJ.** 2012. N-Acylethanolamines and related compounds: aspects of metabolism and functions. *Plant Science* 184, 129-140.

**Del Río, L. A.** 2015. ROS and RNS in plant physiology: an overview. *Journal of Experimental Botany*, 66(10), 2827-2837.

**Dunand, C., Crèvecoeur, M., Penel, C.** 2007. Distribution of superoxide and hydrogen peroxide in Arabidopsis root and their influence on root development: possible interaction with peroxidases. *New Phytologist*, 174(2), 332-341.

**Faure, L., Cavazos, R., Khan, B. R., Petros, R. A., Koulen, P., Blancaflor, E. B., Chapman, K. D.** 2015. Effects of synthetic alkamides on Arabidopsis fatty acid amide hydrolase activity and plant development. *Phytochemistry*, 110, 58-71.

**Fernández-Marcos, M., Desvoyes, B., Manzano, C., Liberman, L. M., Benfey, P. N., Del Pozo, J. C., Gutierrez, C.** 2017. Control of *Arabidopsis* lateral root primordium boundaries by MYB 36. *New Phytologist*, 213(1), 105-112.

**Foreman, J., Demidchik, V., Bothwell, J. H., et al** 2003. Reactive oxygen species produced by NADPH oxidase regulate plant cell growth. *Nature*, 422(6930), 442-446.

**Ghassemian, M., Lutes, J., Chang, H. S., Lange, I., Chen, W., Zhu, T., Wang, X., Lange, B. M.** (2008). Abscisic acid-induced modulation of metabolic and redox control pathways in *Arabidopsis thaliana*. *Phytochemistry*, 69(17), 2899-2911.

**Gertsch, J.** 2008. Immunomodulatory lipids in plants: plant fatty acid amides and the human endocannabinoid system. *Planta Medica*, 74(06), 638-650.

**Hartje, S., Zimmermann, S., Klonus, D., & Mueller-Roeber, B.** 2000. Functional characterisation of LKT1, a K<sup>+</sup> uptake channel from tomato root hairs, and comparison with the closely related potato inwardly rectifying K<sup>+</sup> channel SKT1 after expression in *Xenopus* oocytes. *Planta*, 210(5), 723-731.

**Hayyan, M., Hashim, M. A., & Al Nashef, I. M.** 2016. Superoxide ion: generation and chemical implications. *Chemical Reviews*, 116(5), 3029-3085.

**Ilan, N., Schwartz, A., & Moran, N.** 1996. External protons enhance the activity of the hyperpolarization-activated K channels in guard cell protoplasts of *Vicia faba*. *The Journal of Membrane Biology*, 154(2), 169-181.

**Jaspers, P., Kangasjärvi, J.** 2010. Reactive oxygen species in abiotic stress signaling. *Physiologia Plantarum*, 138(4), 405-413.

**Kagenishi, T., Yokawa, K., Baluška, F.** 2016. MES buffer affects *Arabidopsis* root apex zonation and root growth by suppressing superoxide generation in root apex. *Frontiers in Plant Science*, 7, 79.

**Kravchenko, V. V., Kaufmann, G. F., Mathison, J. C., et al.** 2006. N-(3-oxo-acyl) homoserine lactones signal cell activation through a mechanism distinct from the canonical pathogen-associated molecular pattern recognition receptor pathways. *Journal of Biological Chemistry*, 281(39), 28822-28830.

**Kunos, G., Járαι, Z., Bátkai, S., Goparaju, S. K., Ishac, E. J., Liu, J., Wang, L., Wagner, J. A.** 2000. Endocannabinoids as cardiovascular modulators. *Chemistry and Physics of Lipids*, 108(1-2), 159-168.

**Li, N., Sun, L., Zhang, L., Song, Y., Hu, P., Li, C., Hao, F. S.** 2015. AtrbohD and AtrbohF negatively regulate lateral root development by changing the localized accumulation of superoxide in primary roots of *Arabidopsis*. *Planta*, 241(3), 591-602.

**Liang, X., Ma, M., Zhou, Z., et al.** 2018. Ligand-triggered de-repression of *Arabidopsis* heterotrimeric G proteins coupled to immune receptor kinases. *Cell Research*, 28(5), 529-543.

**Liu, F., Bian, Z., Jia, Z., Zhao, Q., Song, S.** 2012. The GCR1 and GPA1 participate in promotion of *Arabidopsis* primary root elongation induced by N-acyl-homoserine lactones, the bacterial quorum-sensing signals. *Molecular Plant-Microbe Interactions*, 25(5), 677-683.

**Livanos, P., Apostolakos, P., Galatis, B.** 2012. Plant Cell Division: ROS homeostasis is required. *Plant Signaling & Behavior*, 7(7), 771-778.

**López-Bucio, J., Millán-Godínez, M., Méndez-Bravo, A., Morquecho-Contreras, A., Ramírez-Chávez, E., Molina-Torres, J., Pérez-Torres, A., Higuchi, M., Kakimoto T., Herrera-Estrella, L.** 2007. Cytokinin receptors are involved in alkamide regulation of root and shoot development in *Arabidopsis*. *Plant Physiology*, 145(4), 1703-1713.

**Marklund, S.** 1976. Spectrophotometric study of spontaneous disproportionation of superoxide anion radical and sensitive direct assay for superoxide dismutase. *Journal of Biological Chemistry*, 251(23), 7504-7507.

**Manzano, C., Pallero-Baena, M., Casimiro, I., De Rybel, B., Orman-Ligeza, B., Van Isterdael, G., Beeckman, T., Draye, X., Del Pozo, J. C.** 2014. The emerging role of reactive oxygen species signaling during lateral root development. *Plant Physiology*, 165(3), 1105-1119.

**Mathesius, U., Mulders, S., Gao, M., Teplitski, M., Caetano-Anollés, G., Rolfe, B. G., Bauer, W. D.** 2003. Extensive and specific responses of a eukaryote to bacterial quorum-sensing signals. *Proceedings of the National Academy of Sciences*, 100(3), 1444-1449.

**Méndez-Bravo, A., Calderón-Vázquez, C., Ibarra-Laclette, E., Raya-González, J., Ramírez-Chávez, E., Molina-Torres, J., Guevara-García, A.A., López-Bucio, J., Herrera-Estrella, L.** 2011. Alkamides activate jasmonic acid biosynthesis and signaling pathways and confer resistance to *Botrytis cinerea* in *Arabidopsis thaliana*. *PloS One*, 6(11), e27251.

**Méndez-Bravo, A., Raya-González, J., Herrera-Estrella, L., López-Bucio, J.** 2010. Nitric oxide is involved in alkamide-induced lateral root development in *Arabidopsis*. *Plant and Cell Physiology*, 51(10), 1612-1626.

**Micheli, F.** 2001. Pectin methylesterases: cell wall enzymes with important roles in plant physiology. *Trends in Plant Science*, 6(9), 414-419.

**Miller, E. W., Dickinson, B. C., Chang, C. J.** 2010. Aquaporin-3 mediates hydrogen peroxide uptake to regulate downstream intracellular signaling. *Proceedings of the National Academy of Sciences*, 107(36), 15681-15686.

**Miller, A. F.** 2012. Superoxide dismutases: ancient enzymes and new insights. *FEBS letters*, 586(5), 585-595.

**Mittler, R., Vanderauwera, S., Suzuki, N., Miller, G. A. D., Tognetti, V. B., Vandepoele, K., Gollery, M., Shulaev, V., Van Breusegem, F.** 2011. ROS signaling: the new wave? *Trends in Plant Science*, 16(6), 300-309.

**Mittler, R.** 2017. ROS are good. *Trends in Plant Science*, 22(1), 11-19.

**Molinatorres, J., Salgado-Garciglia, R., Ramirez-Chavez, E., Del Rio, R. E.** 1996. Purely olefinic alkamides in *Heliopsis longipes* and *Acmella* (*Spilanthes*) *oppositifolia*. *Biochemical Systematics and Ecology*, 24(1), 43-47.

**Molina-Torres, J., Salazar-Cabrera, C. J., Armenta-Salinas, C., Ramírez-Chávez, E.** 2004. Fungistatic and bacteriostatic activities of alkamides from *Heliopsis longipes* roots: affinin and reduced amides. *Journal of Agricultural and Food Chemistry*, 52(15), 4700-4704.

**Monshausen, G. B., Bibikova, T. N., Weisenseel, M. H., Gilroy, S.** 2009. Ca<sup>2+</sup> regulates reactive oxygen species production and pH during mechanosensing in *Arabidopsis* roots. *The Plant Cell*, 21(8), 2341-2356.

**Ogasawara, Y., Kaya, H., Hiraoka, G., et al.** 2008. Synergistic activation of the *Arabidopsis* NADPH oxidase AtrbohD by Ca<sup>2+</sup> and phosphorylation. *Journal of Biological Chemistry*, 283(14), 8885-8892.

**Orman-Ligeza, B., Parizot, B., De Rycke, R., Fernandez, A., Himschoot, E., Van Breusegem, F., Bennett, M.J., Périlleux, C., Beeckman T., Draye, X.** 2016. RBOH-mediated ROS production facilitates lateral root emergence in *Arabidopsis*. *Development*, 143(18), 3328-3339.

**Ortíz-Castro R, Martínez-Trujillo M, López-Bucio J.** 2008. N-acyl-L-homoserine lactones: a class of bacterial quorum-sensing signals alter post-embryonic root development in *Arabidopsis thaliana*. *Plant, Cell & Environment*, 31(10), 1497-1509.

**Overmyer, K., Brosché, M., & Kangasjärvi, J.** 2003. Reactive oxygen species and hormonal control of cell death. *Trends in Plant Science*, 8(7), 335-342.

**Passardi, F., Tognolli, M., De Meyer, M., Penel, C., Dunand, C.** 2006. Two cell wall associated peroxidases from *Arabidopsis* influence root elongation. *Planta*, 223(5), 965-974.

**Potters, G., Pasternak, T. P., Guisez, Y., Jansen, M. A.** (2009). Different stresses, similar morphogenic responses: integrating a plethora of pathways. *Plant, Cell & Environment*, 32(2), 158-169.

**Prachayasittikul, V., Prachayasittikul, S., Ruchirawat, S., & Prachayasittikul, V.** (2013). High therapeutic potential of *Spilanthes acmella*: a review. *EXCLI journal*, 12, 291.

**Qi, J., Wang, J., Gong, Z., Zhou, J. M.** 2017. Apoplastic ROS signaling in plant immunity. *Current Opinion in Plant Biology*, 38, 92-100.

**Ramírez-Chávez, E., López-Bucio, J., Herrera-Estrella, L., Molina-Torres, J.** 2004. Alkamides isolated from plants promote growth and alter root development in *Arabidopsis*. *Plant Physiology*, 134(3), 1058-1068.

**Rios, M. Y., Olivo, H. F.** 2014. Natural and synthetic alkamides: applications in pain therapy. In: Rahman, E, ed. *Studies in Natural Products Chemistry*. Elsevier. Vol. 43, 79-121.

**Sagi, M., Fluhr, R.** 2006. Production of reactive oxygen species by plant NADPH oxidases. *Plant Physiology*, 141(2), 336-340.

**Schenk, S. T., Stein, E., Kogel, K. H., Schikora, A.** 2012. *Arabidopsis* growth and defense are modulated by bacterial quorum sensing molecules. *Plant Signaling & Behavior*, 7(2), 178-181.

**Schneider, C. A., Rasband, W. S., Eliceiri, K. W.** 2012. NIH Image to ImageJ: 25 years of image analysis. *Nature Methods*, 9(7), 671-675.

**Schuhegger, R., Ihring, A., Gantner, S., et al.** 2006. Induction of systemic resistance in tomato by N-acyl-L-homoserine lactone-producing rhizosphere bacteria. *Plant, Cell & Environment*, 29(5), 909-918.

**Sherrier, D. J., VandenBosch, K. A.** 1994. Secretion of cell wall polysaccharides in *Vicia* root hairs. *The Plant Journal*, 5(2), 185-195.

**Song, S., Jia, Z., Xu, J., Zhang, Z., Bian, Z.** 2011. N-butyryl-homoserine lactone, a bacterial quorum-sensing signaling molecule, induces intracellular calcium elevation in *Arabidopsis* root cells. *Biochemical and Biophysical Research Communications*, 414(2), 355-360.

**Suzuki, N., Miller, G., Morales, J., Shulaev, V., Torres, M. A., Mittler, R.** 2011. Respiratory burst oxidases: the engines of ROS signaling. *Current Opinion in Plant Biology*, 14(6), 691-699.

**Thordal-Christensen, H., Zhang, Z., Wei, Y., Collinge, D. B.** 1997. Subcellular localization of H<sub>2</sub>O<sub>2</sub> in plants. H<sub>2</sub>O<sub>2</sub> accumulation in papillae and hypersensitive response during the barley—powdery mildew interaction. *The Plant Journal*, 11(6), 1187-1194.

**Tognetti, V. B., Mühlenbock, P. E. R., Van Breusegem, F.** 2012. Stress homeostasis—the redox and auxin perspective. *Plant, Cell & Environment*, 35(2), 321-333.

**Torres, M. A., Dangl, J. L., Jones, J. D.** 2002. *Arabidopsis* gp91phox homologues AtrbohD and AtrbohF are required for accumulation of reactive oxygen intermediates in the plant defense response. *Proceedings of the National Academy of Sciences*, 99(1), 517-522.

**Torres, M. A.** 2010. ROS in biotic interactions. *Physiologia Plantarum*, 138(4), 414-429.

**Tripathy, S., Venables, B. J., & Chapman, K. D.** 1999. N-Acylethanolamines in signal transduction of elicitor perception. Attenuation of alkalization response and activation of defense gene expression. *Plant Physiology*, 121(4), 1299-1308.

**Tripathy, S., Kleppinger-Sparace, K., Dixon, R. A., Chapman, K. D.** 2003. N-acylethanolamine signaling in tobacco is mediated by a membrane-associated, high-affinity binding protein. *Plant Physiology*, 131(4), 1781-1791.

**Tsukagoshi, H., Busch, W., Benfey, P. N.** 2010. Transcriptional regulation of ROS controls transition from proliferation to differentiation in the root. *Cell*, 143(4), 606-616.

**Tsukagoshi, H.** 2016. Control of root growth and development by reactive oxygen species. *Current Opinion in Plant Biology*, 29, 57-63.

**Ubeda-Tomás, S., Federici, F., Casimiro, I., Beemster, G. T., Bhalerao, R., Swarup, R., Doerner, P., Haseloff J., Bennett, M. J.** 2009. Gibberellin signaling in the endodermis controls *Arabidopsis* root meristem size. *Current Biology*, 19(14), 1194-1199.

**Urano, D., & Jones, A. M. (2014).** Heterotrimeric G protein–coupled signaling in plants. *Annual Review of Plant Biology*, 65, 365-384.

**von Rad, U., Klein, I., Dobrev, P. I., Kottova, J., Zazimalova, E., Fekete, A., Hartmann, A., Schmitt-Kopplin, P., Durner, J.** 2008. Response of *Arabidopsis thaliana* to N-hexanoyl-DL-homoserine-lactone, a bacterial quorum sensing molecule produced in the rhizosphere. *Planta*, 229(1), 73-85.



**Wang, Y. S., Shrestha, R., Kilaru, A., Wiant, W., Venables, B. J., Chapman, K. D., Blancaflor, E. B.** 2006. Manipulation of *Arabidopsis* fatty acid amide hydrolase expression modifies plant growth and sensitivity to N-acyl ethanolamines. *Proceedings of the National Academy of Sciences*, 103(32), 12197-12202.

**Wilson, R. I., Nicoll, R. A.** 2002. Endocannabinoid signaling in the brain. *Science*, 296(5568), 678-682.

**Yan, C., Cannon, A. E., Watkins, J., Keereetaweep, J., Khan, B. R., Jones, A. M., B Blancaflor, E., Azad, R.K., Chapman, K. D.** 2020. Seedling chloroplast responses induced by N-linolenylethanolamine require intact G-protein complexes. *Plant Physiology*, 184(1), 459-477.

**Zhang, Y., Guo, W. M., Chen, S. M., Han, L., Li, Z. M.** 2007. The role of N-lauroylethanolamine in the regulation of senescence of cut carnations (*Dianthus caryophyllus*). *Journal of Plant Physiology*, 164(8), 993-1001.

**Zandonadi, D. B., Santos, M. P., Dobbss, L. B., Olivares, F. L., Canellas, L. P., Binzel, M. L., Okorokova-Façanha, A.L., Façanha, A. R.** 2010. Nitric oxide mediates humic acids-induced root development and plasma membrane H<sup>+</sup>-ATPase activation. *Planta*, 231(5), 1025-1036.

**Zhang, W., Jeon, B. W., Assmann, S. M.** 2011. Heterotrimeric G-protein regulation of ROS signalling and calcium currents in *Arabidopsis* guard cells. *Journal of Experimental Botany*, 62(7), 2371-2379.

**Zhao, J., Davis, L. C., Verpoorte, R.** 2005. Elicitor signal transduction leading to production of plant secondary metabolites. *Biotechnology Advances*, 23(4), 283-333.

**Zhao, Q., Zhang, C., Jia, Z., Huang, Y., Li, H., Song, S.** 2015. Involvement of calmodulin in regulation of primary root elongation by N-3-oxo-hexanoyl homoserine lactone in *Arabidopsis thaliana*. *Frontiers in Plant Science*, 5, 807.

**Zhao, Y., Zhang, Y., Liu, F., Wang, R., Huang, L., & Shen, W.** 2019. Hydrogen peroxide is involved in methane-induced tomato lateral root formation. *Plant Cell Reports*, 38(3), 377-389.

**Table 1. N-acyl amides in plant development**

Type	Chain length: insaturations	Activity	Reference
NAE	12:00	Flower senescence: Increase activity of SOD, Cat, APX and GR.	Zhang <i>et al.</i> , 2007
NAE	12:00	Reduction of: primary root growth, secondary roots, root hair formation, apex swelling, cell invaginations of the plasma membrane, increase levels of vesicles at the cell periphery, improper cell walls near the meristematic region, disorganize endomembrane system and alter vesicular trafficking. Increase the expression of ABRE genes	Blancaflor <i>et al.</i> , 2003
NAE	12:0 to 18:3	Inhibition of PLD $\alpha$ activity	Austin-Brown and Chapman, 2002
NAE	12:0, 18:3	Reduction of root elongation rate.	Wang <i>et al.</i> , 2010; Blancaflor <i>et al.</i> , 2003
NAE	12:0, 14:0, 18:0, 18:1, 18:3, 20:4	Plant defense: Inhibit alkalization of the extracellular medium, modulate the ion flux in the plasma membrane and Induce PAL expression.	Tripathy <i>et al.</i> , 1999; Tripathy <i>et al.</i> , 2003
NAE	12:0, 18:2	Interacts with the ABA signaling pathway to elicit secondary dormancy	Blancaflor <i>et al.</i> , 2014; Wang <i>et al.</i> , 2006
AHL	C4-HSL	Intracellular Ca <sup>2+</sup> elevation	Song <i>et al.</i> , 2011
AHL	C4-HSL, C6-HSL, C8-HSL	Increase primary root growth and plant biomass. Resistance against necrotrophic pathogens. Increase SA-levels and defense-gene regulation.	Liu <i>et al.</i> , 2012; Schenk <i>et al.</i> , 2012; von Rad <i>et al.</i> , 2008; Schuhegger <i>et al.</i> , 2006
AHL	C6-HSL	Alteration in auxin/cytokinin level and herbivore susceptibility	von Rad <i>et al.</i> , 2008; Schenk <i>et al.</i> , 2012;
AHL	C10-HSL, C12-HSL	Inhibition of primary root growth.	Zhao <i>et al.</i> , 2015

## Figure legends

**Figure. 1. Effect of affinin on root architecture in *Arabidopsis* Col-0 accession.** (A) Plants grown on affinin treatments (Bars=1cm); (B) primary root length ( $n=10$ ); (C) number of emerged lateral roots ( $n=10$ ) and (D) root hair length ( $n=10$ ). (E, H) confocal images of the primary root from tip to first root hair bulge (Bars=0.1mm), (F, I) confocal images of cells from the elongation-differentiation zone (Bars=0.05mm); (G, J) confocal images of apical meristem size. White arrows indicate root hair bulge and grey arrows shows the transition zone (Bars=0.05mm). (K) Shows the mean distance from QC to the first root hair bulge ( $n=5$ ), (L) is the mean value of cell length in the elongation/differentiation zone ( $n=3$ ) and (M) shows the mean value of the apical meristem length ( $n=5$ ). Data was analysed with one-way ANOVA followed by a Tukey test using the InfoStat software ([www.infostat.com.ar](http://www.infostat.com.ar)) Different lower-case letters are used to indicate means that differ significantly ( $P \leq 0.05$ ). Micrographs were adjusted with the same settings; Colour saturation: 0%, Brightness: 40% and Contrast: 40%

**Figure.2. Affinin induced root-developmental changes are mediated by ROS.** (A) Detection of endogenous  $H_2O_2$  accumulation with 3, 3'-diaminobenzidine (DAB) staining and (B) nitroblue tetrazolium (NBT) staining, visualizing superoxide ( $O_2^{\cdot-}$ ) accumulation of primary roots treated with affinin (Bars=300 $\mu$ m). (C) Visualization of *in situ* accumulation of endogenous  $H_2O_2$  using DAB staining in root apical meristem (Bars=100 $\mu$ m) and lateral root emerging sites (Bars=50 $\mu$ m) of Col-0 wild type plants. Data shown in (D) represent the mean  $\pm$  SE of  $H_2O_2$  staining intensity measured in (C). (E) Affinin-induced *Arabidopsis* (Col-0) lateral rooting is sensitive to synthetic inhibitor of flavoenzymes, diphenyleneiodonium (DPI), used here to target NAD(P)H oxidases (Bars=1cm). Data shown in (F) represent the mean  $\pm$  SE of emerged lateral root number measured in (E). Data in (D) was analysed with one-way ANOVA ( $n=10$ ) and a Tukey test using the InfoStat software ([www.infostat.com.ar](http://www.infostat.com.ar)). Data in (F) was analysed with two-way ANOVA ( $n=10$ ) and a Tukey test using Minitab software (<https://www.minitab.com/>). Different lower-case letters are used to indicate means that differ significantly ( $P \leq 0.05$ ). Micrographs were adjusted with the same settings; Colour saturation: 0%, Brightness: 0% and Contrast: 20%.

**Figure 3. Effect of affinin on root system architecture in the class III peroxidase mutant *Arabidopsis peroxidase34* (*prx34*).** (A) Represents the mean  $\pm$  SE of primary root length ( $n=10$ ) while (B) is the number of emerged lateral roots ( $n=10$ ) of plants grown in different affinin treatments. (C) Visualization of *in situ* accumulation of endogenous  $H_2O_2$  using 3, 3'-diaminobenzidine (DAB) staining in root apical meristem (Bars=100 $\mu$ m) and lateral root emerging sites (Bars=50 $\mu$ m) of *prx34* mutant plants. Data shown in (D) represent the mean  $\pm$  SE of  $H_2O_2$  staining intensity measured in (C). Data was analysed with two-way ANOVA ( $n=10$ ) and a Tukey test using Minitab software (<https://www.minitab.com/>). Different lower-case letters are used to indicate means that differ significantly ( $P \leq 0.05$ ). Micrographs were adjusted with the same settings; Colour saturation: 0%, Brightness: 0% and Contrast: 20%.

**Figure 4. RESPIRATORY BURST OXIDASE HOMOLOG (RBOH) mediated ROS production is involved in root developmental changes induced by affinin.** Data shown in (A) represent the mean  $\pm$  SE of primary root length ( $n=10$ ) while data shown in (B) represent the mean  $\pm$  SE of emerged lateral roots ( $n=10$ ). (C) DAB staining of root tips and lateral root primordia surrounding area (D). Data in (E) represent the mean  $\pm$  SE of  $H_2O_2$  staining intensity in root tips ( $n=10$ ) and (F) in lateral root primordia surrounding area ( $n=10$ ). Photographs in (G) shown the representative morphology of root hairs, while data shown in (H) represent the mean  $\pm$  SE of root hair length measured in (G) ( $n=10$ ). Data was analysed with two-way ANOVA ( $n=10$ ) and a Tukey test using Minitab software (<https://www.minitab.com/>). Different lower-case letters are used to indicate means that differ significantly ( $P \leq 0.05$ ). Micrographs were adjusted with the same settings; Colour saturation: 0%, Brightness: 0% and Contrast: 20%.

**Figure 5. Effect of affinin on root growth of *Arabidopsis* heterotrimeric G-protein subunit mutants.** Data shown in (A) represent the mean  $\pm$  SE of primary root length ( $n=10$ ) and (B) the emerged lateral roots number ( $n=10$ ) from heterotrimeric G-protein mutants while (C) represent the mean  $\pm$  SE of primary root length ( $n=10$ ) and (D) the emerged lateral roots number ( $n=10$ ) from the regulator of G-protein mutant. Data was analysed with two-way ANOVA ( $n=10$ ) and a Tukey test using Minitab software (<https://www.minitab.com/>). Different lower-case letters are used to indicate means that differ significantly ( $P \leq 0.05$ ).

**Figure 6. Involvement of extracellular pH change in affinin-induced developmental responses.** (A) Rhizosphere acidification in the maturation zone of *Arabidopsis* roots in response to different affinin treatments (Bars=1cm); the scale on the left is a pH reference scale in the agarose without plants. Data shown in (B) represent the mean  $\pm$  SE of medium pH measured in a region of interest (ROI) near the roots of seedlings ( $n=7$ ). (C) Photographs of full seedlings (Bars=1cm) and (F) root hairs (Bars=0.5mm) of plants treated with or without affinin grown in a medium containing or lacking MES buffer ( $0.5\text{g L}^{-1}$ ). Data shown represent the mean  $\pm$  SE of primary root length (D), emerged lateral roots (E) and root hair length (G) ( $n=10$ ). Data was analysed with two-way ANOVA and a Tukey test using Minitab software (<https://www.minitab.com/>). Different lower-case letters are used to indicate means that differ significantly ( $P \leq 0.05$ ). Micrographs were adjusted with the same settings; Colour saturation: 0%, Brightness: 0% and Contrast: 20%.

## Figures

Figure 1

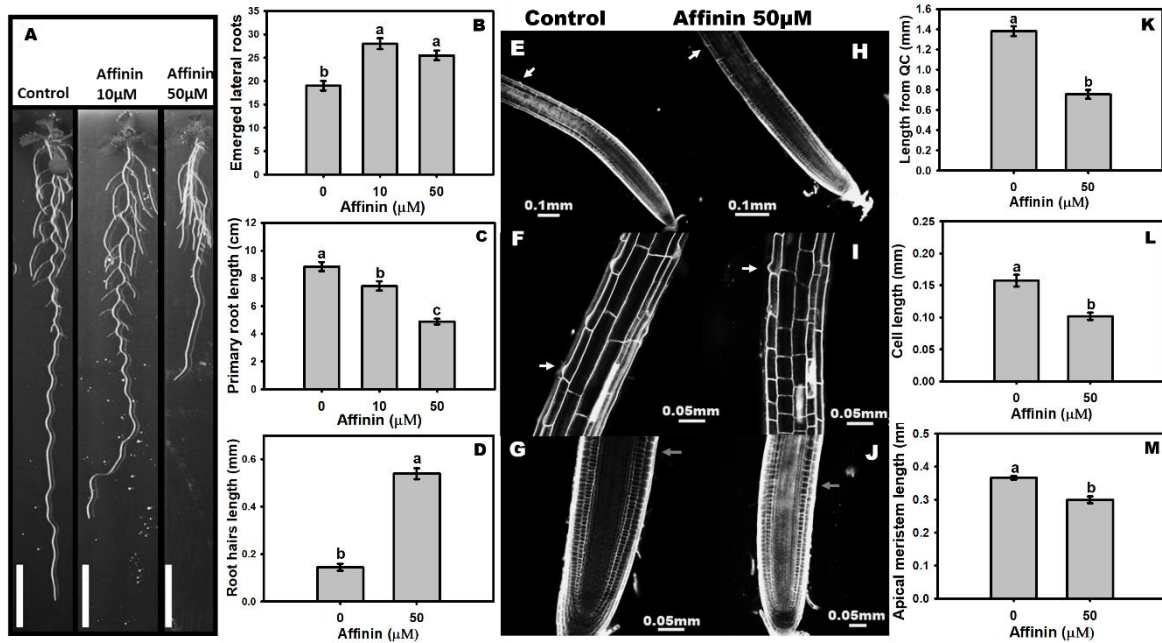


**Fig. 1.** Effect of affinin on root architecture in *Arabidopsis Col-0* accession. (A) Plants grown on affinin treatments (Bars=1cm); (B) primary root length ( $n=10$ ); (C) number of emerged lateral roots ( $n=10$ ) and (D) root hair length ( $n=10$ ). (E, H) confocal images of the primary root from tip to first root hair bulge (Bars=0.1mm), (F, I) confocal images of cells from the elongation-differentiation zone (Bars=0.05mm); (G, J) confocal images of apical meristem size. White arrows indicate root hair bulge and grey arrows shows the transition zone (Bars=0.05mm). (K) Shows the mean distance from QC to the first root hair bulge ( $n=5$ ), (L) is the mean value of cell length in the elongation/differentiation zone ( $n=3$ ) and (M) shows the mean value of the apical meristem length ( $n=5$ ). Data was analysed with one-way ANOVA followed by a Tukey test using the InfoStat software ([www.infostat.com.ar](http://www.infostat.com.ar)) Different lower-case letters are used to indicate means that differ significantly ( $P \leq 0.05$ ). Micrographs were adjusted with the same settings; Colour saturation: 0%, Brightness: 40% and Contrast: 40%



**Figure 2**

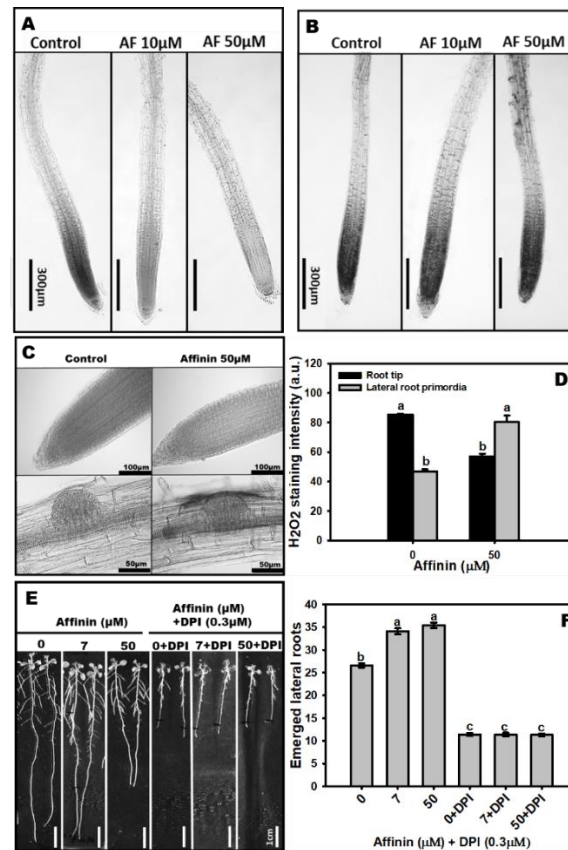


**Fig. 2.** Affinin induced root-developmental changes are mediated by ROS. (A) Detection of endogenous H<sub>2</sub>O<sub>2</sub> accumulation with 3, 3'-diaminobenzidine (DAB) staining and (B) nitroblue tetrazolium (NBT) staining, visualizing superoxide (O<sub>2</sub><sup>-</sup>) accumulation of primary roots treated with affinin (Bars=300μm). (C) Visualization of *in situ* accumulation of endogenous H<sub>2</sub>O<sub>2</sub> using DAB staining in root apical meristem (Bars=100μm) and lateral root emerging sites (Bars=50μm) of Col-0 wild type plants. Data shown in (D) represent the mean ± SE of H<sub>2</sub>O<sub>2</sub> staining intensity measured in (C). (E) Affinin-induced *Arabidopsis* (Col-0) lateral rooting is sensitive to synthetic inhibitor of flavoenzymes, diphenyleneiodonium (DPI), used here to target NAD(P)H oxidases (Bars=1cm). Data shown in (F) represent the mean ± SE of emerged lateral root number measured in (E). Data in (D) was analysed with one-way ANOVA ( $n=10$ ) and a Tukey test using the InfoStat software ([www.infostat.com.ar](http://www.infostat.com.ar)). Data in (F) was analysed with two-way ANOVA ( $n=10$ ) and a Tukey test using Minitab software (<https://www.minitab.com/>). Different lower-case letters are used to indicate means that differ significantly ( $P \leq 0.05$ ). Micrographs were adjusted with the same settings; Colour saturation: 0%, Brightness: 0% and Contrast: 20%.

**Figure 3**

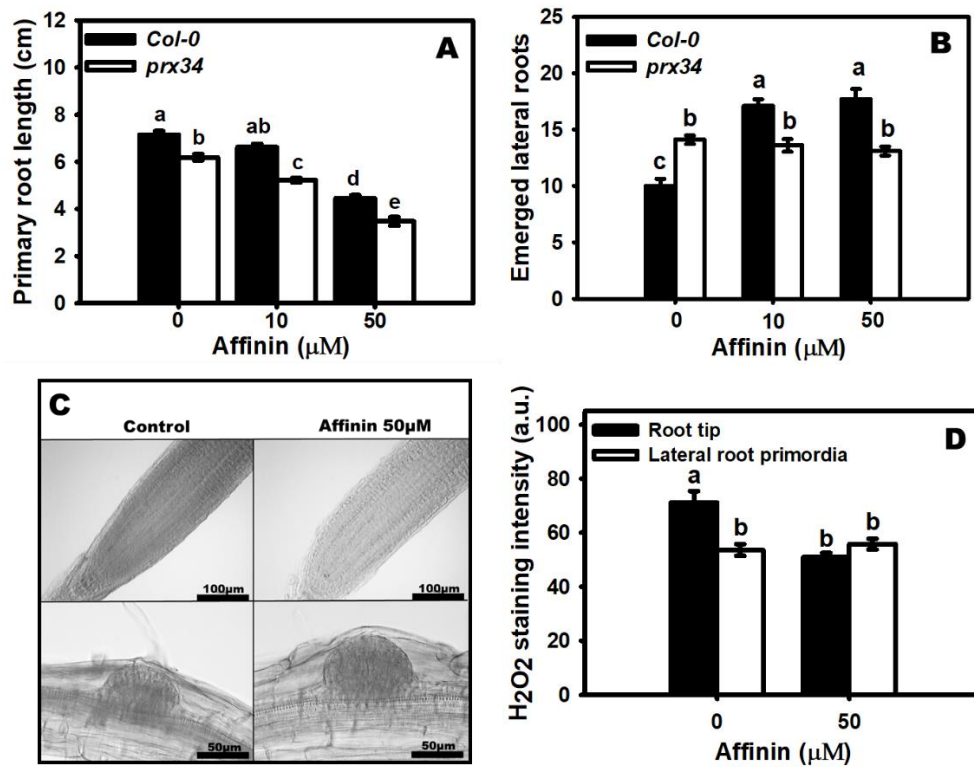


**Fig. 3.** Effect of affinin on root system architecture in *Arabidopsis peroxidase34* (*prx34*) class III peroxidase mutant. (A) represents the mean  $\pm$  SE of primary root length ( $n=10$ ) while (B) is the number of emerged lateral roots ( $n=10$ ) of plants grown in different affinin treatments. (C) Visualization of *in situ* accumulation of endogenous H<sub>2</sub>O<sub>2</sub> using 3, 3'-diaminobenzidine (DAB) staining in root apical meristem (Bars=100 $\mu\text{m}$ ) and lateral root emerging sites (Bars=50 $\mu\text{m}$ ) of *prx34* mutant plants. Data shown in (D) represent the mean  $\pm$  SE of H<sub>2</sub>O<sub>2</sub> staining intensity measured in (C). Data was analysed with two-way ANOVA ( $n=10$ ) and a Tukey test using Minitab software (<https://www.minitab.com/>). Different lower-case letters are used to indicate means that differ significantly ( $P \leq 0.05$ ). Micrographs were adjusted with the same settings; Colour saturation: 0%, Brightness: 0% and Contrast: 20%.

**Figure 4**

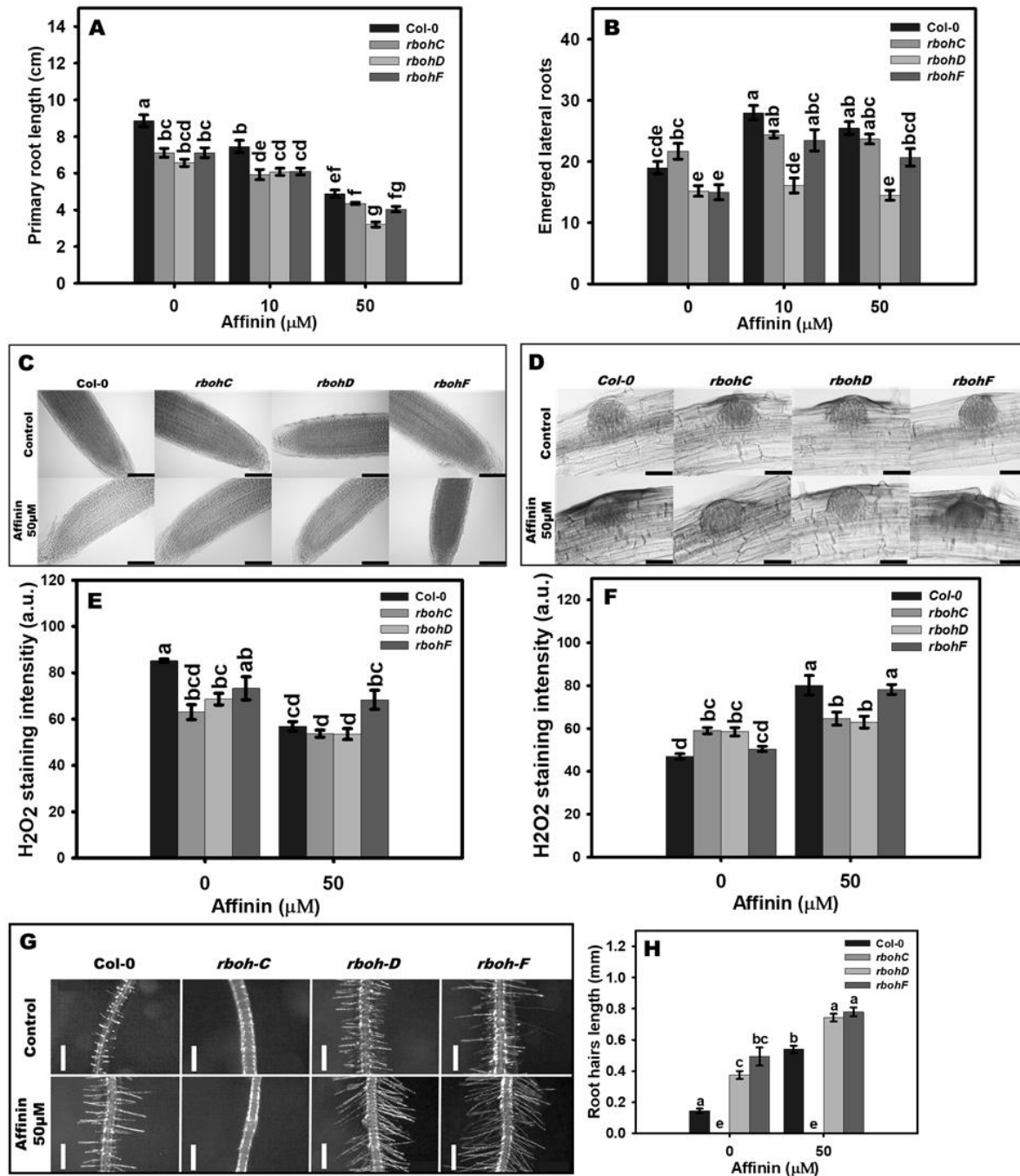


**Fig. 4.** RESPIRATORY BURST OXIDASE HOMOLOG (RBOH) mediated ROS production is involved in root developmental changes induced by affinin. Data shown in (A) represent the mean  $\pm$  SE of primary root length ( $n=10$ ) while data shown in (B) represent the mean  $\pm$  SE of emerged lateral roots ( $n=10$ ). (C) DAB staining of root tips and lateral root

primordia surrounding area (D). Data in (E) represent the mean  $\pm$  SE of H<sub>2</sub>O<sub>2</sub> staining intensity in root tips ( $n=10$ ) and (F) in lateral root primordia surrounding area ( $n=10$ ). Photographs in (G) shown the representative morphology of root hairs, while data shown in (H) represent the mean  $\pm$  SE of root hair length measured in (G) ( $n=10$ ). Data was analysed with two-way ANOVA ( $n=10$ ) and a Tukey test using Minitab software (<https://www.minitab.com/>). Different lower-case letters are used to indicate means that differ significantly ( $P \leq 0.05$ ). Micrographs were adjusted with the same settings; Colour saturation: 0%, Brightness: 0% and Contrast: 20%.

**Figure 5**

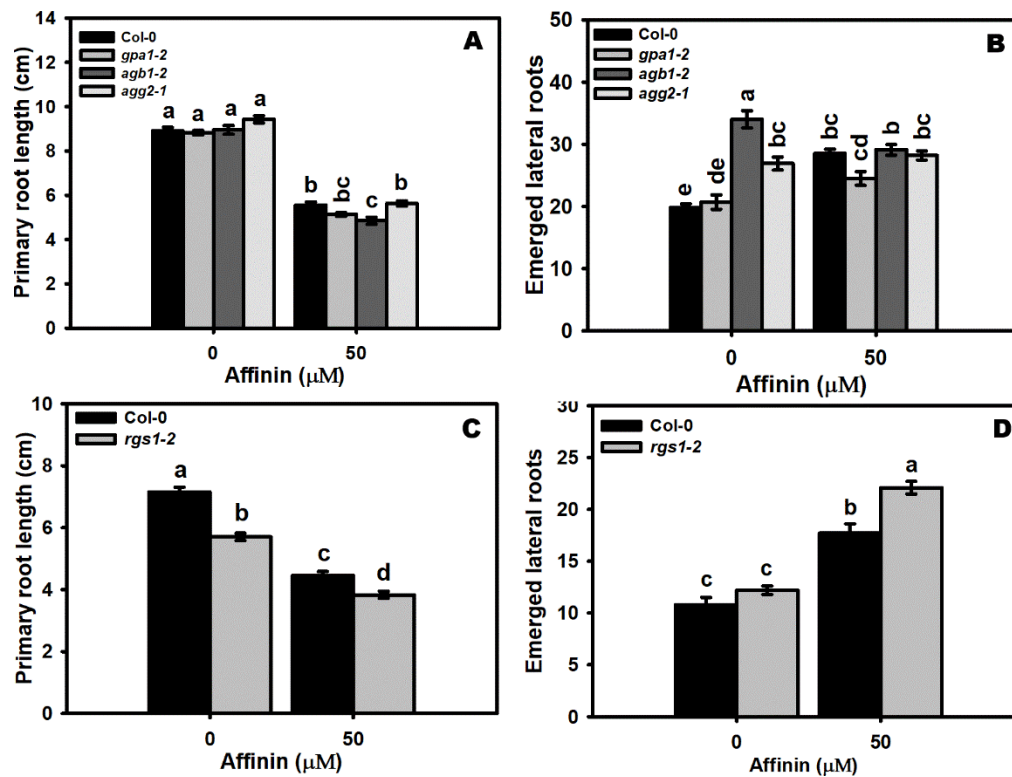


**Figure 5.** Effect of affinin on root growth of *Arabidopsis* heterotrimeric G-protein subunits mutants. Data shown in (A) represent the mean  $\pm$  SE of primary root length ( $n=10$ ) and (B) the emerged lateral roots number ( $n=10$ ) from heterotrimeric G-protein mutants while (C) represent the mean  $\pm$  SE of primary root length ( $n=10$ ) and (D) the emerged lateral roots number ( $n=10$ ) from the regulator of G-protein mutant. Data was analysed with two-way ANOVA ( $n=10$ ) and a Tukey test using Minitab software (<https://www.minitab.com/>). Different lower-case letters are used to indicate means that differ significantly ( $P \leq 0.05$ ).

**Figure 6**

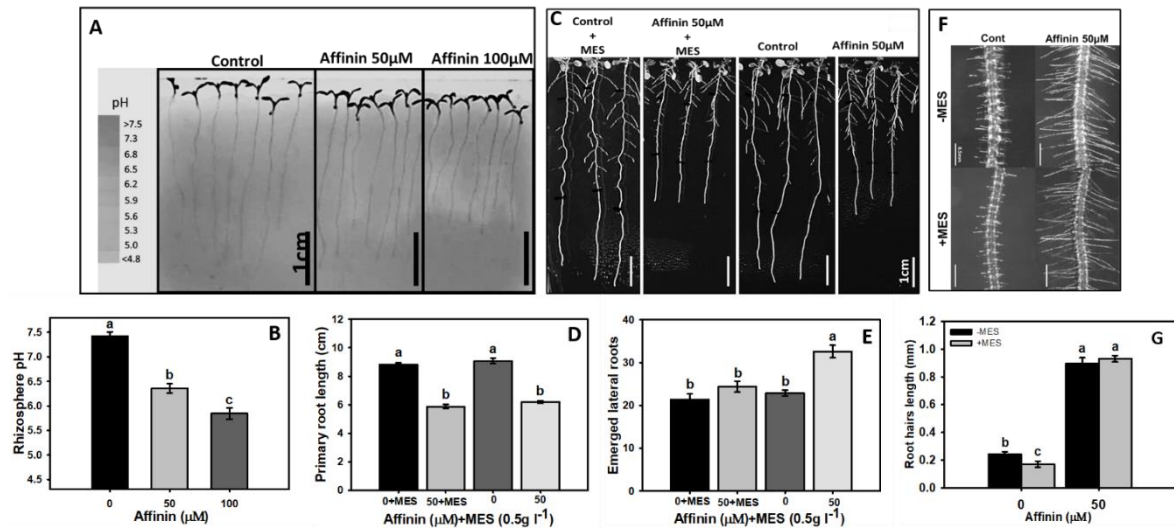


**Figure 6.** Involvement of extracellular pH change in affinin-induced developmental response. (A) Rhizosphere acidification in the maturation zone of *Arabidopsis* roots in response to different affinin treatments (Bars=1cm); the scale on the left is a pH reference scale in the agarose without plants. Data shown in (B) represent the mean  $\pm$  SE of medium pH measured in a region of interest (ROI) near the roots of seedlings ( $n=7$ ). (C) Photographs of full seedlings (Bars=1cm) and (F) root hairs (Bars=0.5mm) of plants treated with or without affinin grown in a medium containing or lacking MES buffer ( $0.5\text{g L}^{-1}$ ). Data shown represent the mean  $\pm$  SE of primary root length (D), emerged lateral roots (E) and root hair length (G) ( $n=10$ ). Data was analysed with two-way ANOVA and a Tukey test using Minitab software (<https://www.minitab.com/>). Different lower-case letters are used to indicate means that differ significantly ( $P \leq 0.05$ ). Micrographs were adjusted with the same settings; Colour saturation: 0%, Brightness: 0% and Contrast: 20%.